Journal of Power Sources 245 (2014) 908–914

Contents lists available at SciVerse ScienceDirect

Journal of Power Sources

journal homepage: www.elsevier.com/locate/jpowsour

Investigating the activity enhancement on Pt_xCo_{1-x} alloys induced by a combined strain and ligand effect

Ioannis Spanos [a,*], Jacob J.K. Kirkensgaard [b], Kell Mortensen [b], Matthias Arenz [a,*]

[a] Nano-science Center, Department of Chemistry, University of Copenhagen, Universitetsparken 5, DK-2100 Copenhagen Ø, Denmark
[b] Niels Bohr Institute, University of Copenhagen, Universitetsparken 5, DK-2100 Copenhagen Ø, Denmark

HIGHLIGHTS

- Different impregnation protocols for the preparation of fuel cell catalysts were investigated.
- The thermal treatment of Pt bimetallic alloys enhances their catalytic activity.
- The particle size distributions established by TEM and SAXS are compared to each other.
- SAXS proved to be a very useful tool for the determination of the particle size distribution.
- A combination of strain and ligand effects enhances the electrocatalytic activity of the catalysts.

GRAPHICAL ABSTRACT

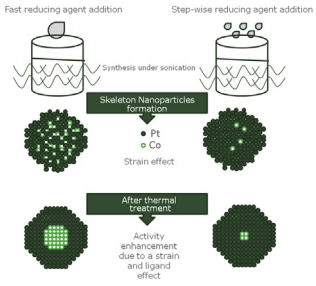

ARTICLE INFO

Article history:
Received 26 April 2013
Received in revised form
2 July 2013
Accepted 5 July 2013
Available online 12 July 2013

Keywords:
PEMFCs
ORR
Pt-alloys
Strain effect
Ligand effect

ABSTRACT

Due to their high activity for the oxygen reduction reaction (ORR), Pt based alloys are of considerable interest as catalysts for polymer electrolyte fuel cells (PEMFC). We present two synthesis protocols that give Pt_xCo_{1-x} alloy nanoparticles (NPs) supported on a commercial carbon black support (Ketjen black EC300J) with controlled particle size, Co content and particle distribution for oxygen reduction reaction (ORR). The as prepared catalysts samples can be pre-leached in acid solution to obtain skeleton NPs and heat-treated in a reducing atmosphere to promote alloying as well as to reduce the number of low coordinated surface sites of the NPs. Without heat treatment, the catalysts exhibit an activity increase for the oxygen reduction reaction mainly due to a strain effect, whereas an improved performance due to a combined strain and ligand effect requires thermal treatment of the catalyst.

1. Introduction

Proton Exchange Membrane Fuel Cells (PEMFCs) are an alternative means for converting chemical into electrical energy. The main advantages over traditional energy converters like automotive engines are the higher conversion efficiency as well as the fact that – if hydrogen from a renewable source is used as fuel – the only product is pure water. However, applications like automotive transport demand the reduction of the cost of fuel cell catalysts, which can in part be achieved by reducing the amount Pt used in the catalyst layer. A more cost effective solution as compared to pure Pt would be alloying Pt with a transition metal (Ni, Co, Fe etc.). For this reason, recently Pt_xCo_{1-x} alloys have attracted considerable

* Corresponding authors.
E-mail addresses: ioaspanos@chem.ku.dk (I. Spanos), m.arenz@chem.ku.dk (M. Arenz).

0378-7753/$ – see front matter © 2013 Elsevier B.V. All rights reserved.
http://dx.doi.org/10.1016/j.jpowsour.2013.07.023

interest as catalysts in PEMFCs due to their superior electrocatalytic properties over Pt for catalysing the Oxygen Reduction Reaction (ORR) [1–4]. The main aim in replacing Pt by Pt-alloys is to decrease the amount of Platinum used in the catalyst in order to alleviate its high cost, but also to increase the reaction rates (activity) and thus enable higher power densities for automotive applications [5].

A variety of techniques are being used for the synthesis of carbon supported Pt alloy NPs, with the most common ones being the impregnation (precipitation) approach [6], which was used for this work, and the incipient wetness approach [7]. The latter is a specific impregnation technique, whereby the active metal precursor is dissolved into a suitable solvent and then contacted with a specific amount of support (high surface area carbon). The essential characteristic is that the volume of the dissolved precursor equals the pore volume of the carbon support. Capillary action then draws the solution into the pores of the support until they are fully saturated, after which the carbon support material begins to appear incipiently wet. A number of processes including selective adsorption, ion exchange and polymerisation/depolymerisation may take place. Then the product is dried and heated (calcined) to remove any excess solvent and decomposes the metal salts into metal oxides. Finally the catalysts may be reduced to convert the metal oxide [8].

The impregnation (precipitation) technique used here is similar to incipient wetness technique, however, an excess of solvent is used during the synthesis, which renders the process slow, because the metal deposition becomes a diffusion process, which is much slower than the capillary one. In order to increase the reaction rate and to convert the metal salts into metallic NPs, a reducing agent (e.g. $NaBH_4$) is typically introduced. Therefore the particle formation involves two distinct processes, namely nucleation (seed formation) and growth. Nucleation requires that the system is far from equilibrium, i.e. high supersaturation or for ionic species a solubility product far exceeding the solubility constant of the solid to be precipitated. Growth of the new phase takes place during conditions which gradually approach the equilibrium state. After synthesis, the excess solvent is separated from the catalyst (precipitate), e.g. by centrifugation. Finally the as prepared catalyst can be further heat treated to decompose any remaining organics and in the case of alloys, to enhance the alloying. Alternatively, a colloidal approach can be used, where Pt or Pt-alloy NPs are preformed in a colloid solution and later attached to the support [9].

Synthesis of Pt_xCo_{1-x} alloy Nanoparticles (NPs) by using an impregnation method can yield NPs with high ORR activity and tunable Pt content as well as particle size [10–13]. Moreover, leaching of the excess surface Co roughens the surface of the NPs leading to a Pt-skeleton surface [1,2]. Heat treatment of the NPs increases the particle size, but can also induce Pt segregation to the surface and the formation of Pt(shell)–Co(core) structures. A strain effect [14] induced from the particle core to the Pt shell can further increase the activity of the catalyst [15].

While all these effects are widely discussed, it is not exactly known how variations in the synthesis protocol influence these effects in a controlled manner and thus allow a fine-tuning of the catalytic behaviour of the catalyst. The knowledge of which approach leads to optimized results is mainly based on trial and error and largely descriptive. In this work we therefore focused on how variations of impregnation – a traditional synthesis method – affect these parameters on carbon supported Pt_xCo_{1-x} NPs. In particular, we studied the manner in which acid leaching and heat treatments change the particle composition and enhance the activity.

2. Experimental

For the synthesis of carbon supported Pt_xCo_{1-x} NPs, 0.052 mmol of K_2PtCl_4 and 0.052 mmol $CoCl_2 \cdot 6H_2O$ were dissolved in 5 ml Ethylene Glycol (EG) each. Then the solutions were ultrasonicated and purged with Ar to remove any oxygen traces. 40 mg of EC300J Ketjen black (Akzo Nobel) high surface area carbon support was added to 10 ml of EG and ultrasonicated to disperse the carbon powder under Ar flow while the pH of the solution was increased to 10 by the addition of NH_4OH. Subsequently, a very small amount (0.2 ml) Pt precursor and 2 ml of a freshly prepared 0.1 M solution of $NaBH_4$ as a reducing agent were added to the carbon suspension under sonication in order to reduce the Pt precursor and form Pt seeds. After 2 min the remaining Pt and Co precursor solutions and a freshly prepared 10 ml solution of $NaBH_4$ were added to the suspension. This method will in the following be denoted as method I. In method II, instead of adding the remaining Pt and Co precursor as well as the $NaBH_4$ solutions at once after the seed formation, the solutions were added in a stepwise fashion until all the Pt and Co precursors were used. In detail, after the seed formation, 1 ml of the Pt and Co precursor solutions were added drop wise to the carbon suspension within a few seconds, followed by the addition of 2 ml of 0.1 M $NaBH_4$ solution. After 2 min of reaction and sonication, this procedure was repeated for another 4 times until all the Pt and Co precursor solutions and the $NaBH_4$ solution were used. Sonication was used through the whole catalyst synthesis procedure. Finally, the catalyst suspension was further sonicated for 2 h under Ar flow. The final product was fine black powder with 20 wt. % Pt loading.

The untreated catalysts were copiously washed with water, these catalysts will be denoted as unleached/PtCo/C(I) and (II) respectively. In the cases denoted as leached (leached/PtCo/C), the as-synthesized catalyst was centrifuged and washed in HCl to remove the excess ethylene glycol and to leach out the surface Co from the NPs. Optionally the leached catalysts were heat treated (HT) in reducing atmosphere (4%H_2–96%Ar) at 500 °C for 30 min, to enhance the alloying and reduce low-coordinated surface sites, denoted as leached/HT PtCo/C(I) and (II).

The electrochemical characterization of the catalysts was conducted in a three-electrode electrochemical cell with a glassy carbon (GC) rotating disk electrode (RDE, 5 mm in diameter) as a working electrode (WE), a Pt-mesh as the counter electrode (CE), a Saturated Calomel Electrode (SCE) as reference electrode (RE), and a home-build potensiostat [16,17]. In order to obtain a thin catalyst film on the GC WE the catalyst powders were dissolved in Millipore water and a known quantity of catalyst ink was pipetted onto the GC electrode, to obtain a Pt loading of 14 $\mu g_{Pt}\ cm^{-2}$. Thereafter the ink was left to dry on the GC electrode under a N_2 stream. As in our previous work, no Nafion binder was necessary for the catalyst ink to adhere on the GC electrode, since no catalyst was visibly detected in the electrolyte solution after the electrochemical measurements. During the electrochemical measurements, the WE potential was compensated for the IR drop to obtain a residual resistance of less than 3 Ω. All potentials are given with respect to the reversible hydrogen electrode (RHE) potential, which was experimentally determined before each measurement series.

The oxygen reduction reaction (ORR) activity was determined in 0.1 M $HClO_4$ prepared from Millipore® water (>18.3 MΩ cm, TOC < 5 ppb) and $HClO_4$ (Merck suprapur). The measurements were performed at room temperature. Prior to the measurements the electrolyte was de-aerated by purging with Ar gas (99.998%, Air Liquide), and the measurements were started with cleaning the catalyst by potential cycles between 0.05 and 1.1 V_{RHE} at a scan rate of 50 mV s^{-1}. The specific activity of the ORR was determined in accordance to our previous work [18] from the positive going RDE polarization curves recorded in O_2 saturated 0.1 M $HClO_4$ solution at a scan rate of 50 mV s^{-1} and at a rotation speed of 1600 rpm. The polarization curves were corrected for the non-faradaic background by subtracting the CVs recorded in Ar-purged electrolyte.

The electrochemical surface area (ECSA) of the catalysts was determined from the CO stripping charge recorded at a sweep rate of 50 mV s^{-1}.

Transmission Electron Microscope micrographs (Tecnai T20 G2 S-TEM Microscope, at 200 kV) of the as-prepared catalysts were recorded in order to study the particle size distribution of the NPs and their distribution on the carbon support. Electron Dispersive X-ray Spectroscopy (EDS) and Inductively Coupled Plasma Mass Spectroscopy (ICP-MS) were used to determine the Pt:Co ratio of the NPs.

The Platinum particle size distribution of the supported catalysts was further determined by X-ray Scattering using a SAXSLab instrument (JJ-Xray, Denmark) equipped with a Rigaku 100XL+ micro focus sealed X-ray tube and a Dectris 2D 300 K Pilatus detector. On this instrument, the detector is moveable allowing different q-ranges to be accessed for the measurement of both Small-Angle and Wide-Angle X-ray Scattering (SAXS/WAXS). Here the magnitude of the scattering vector is defined as $q = 4\pi/\lambda\sin(\theta)$ with λ being the X-ray wavelength and θ half of the scattering angle. Samples were sealed between two 5–7 μm thick mica windows and measurements were performed *in vacuo*. The analysis of the particle size distribution follows [19] with small modifications; for details see Ref. [20]. From each particle size distribution $p(r)$, we calculated a volume normalized surface area of each catalyst by using the following equation:

$$\frac{A}{V} = \frac{\sum_i p(r_i) 4\pi r_i^2}{\sum_i p(r_i) \frac{4\pi}{3} r_i^3}$$

Assuming mass is proportional to volume, the ratios of these areas are directly compared to the ratios of the ECSA and the surface area calculated from the TEM images (histograms). Further, by dividing this ratio with the Platinum density of 21.45 g cm^{-3} absolute numbers per unit mass can be obtained for each sample. The presented model fits are computed using home-written MATLAB code. The results of the SAXS data are shown in Table 1. Lattice constants were determined from peak positions from the WAXS (see Figure S1 in Supplementary information).

3. Results and discussion

3.1. Physical characterization

We start the discussion with the physical characterization of the carbon supported Pt_xCo_{1-x} catalysts that were pre-leached in a controlled manner. TEM micrographs of the catalysts are shown in Fig. 1; the corresponding histograms of the particle size distribution together with the size distribution determined by SAXS are shown in Fig. 2. It is seen that TEM and SAXS data indicate the same trend for the particle size distribution, which lends strong support to the reliability of SAXS as a tool for the determination of the ECSA, as is shown by the comparison of the surface area ratios calculated from electrochemistry measurements, TEM and SAXS (see Table 1). For non-heat treated samples though, the distributions obtained by TEM are shifted towards slightly higher values as compared to the SAXS analysis [21,22]. At this point, the reason for the observed shift in the particle size distribution obtained by TEM and SAXS is not entirely clear. The shift might be related to the synthesis method or the fact the alloy particles are studied as we have not observed such a difference in a previous study of Pt catalysts prepared by a colloidal approach [20]. Furthermore, the observed trend might be due to the limited contrast between the NPs and the support as well as the limited resolution of small NPs in TEM micrographs taken at a relative low resolution to obtain an overview. Being a local method, even with extremely elaborate TEM image analysis the difficult identification of the particle edge may lead to a significant over- or underestimation of particle size. A combination of TEM and SAXS, on the other hand, provides a complete picture of the structural properties of the catalysts both on local and overall scale. Therefore, we used both techniques for our catalyst characterization.

Table 1
Comparison of surface area ratios determined from CO stripping, TEM and SAXS.

Ratio	ECSA	SAXS	TEM
Leached/PtCo/C(I)/leached/PtCo/C(II)	0.78	0.75	0.74
Leached/PtCo/C(I)/leached/HT PtCo/C(I)	1.15	1.12	1.38
Leached/PtCo/C(II)/leached/HT PtCo/C(II)	1.1	1.24	1.6
Leached/HT PtCo/C(I)/leached/HT PtCo/C(II)	0.74	0.83	0.86
Leached/PtCo/C(I)/leached/HT PtCo/C(II)	0.85	0.93	1.18
Leached/PtCo/C(II)/leached/HT PtCo/C(I)	1.48	1.5	1.86

3.1.1. Influence of reducing agent addition

The results from TEM and SAXS show that the Pt_xCo_{1-x} NPs obtained from both impregnation protocols, methods I and II, are well-distributed on the carbon support and exhibit high dispersion. Comparing both impregnation methods, i.e. a fast addition of the metal precursors to the carbon suspension (I) with a step-wise fashion (II), it can be seen that the latter is favourable for obtaining a well defined alloy catalysts. That is, although the average particle size of both catalysts is similar, the leached Pt_xCo_{1-x} NPs (no further heat treatment) of method II have a more uniform size distribution than the ones obtained by method I. TEM and SAXS indicate that the catalyst prepared by method II lacks agglomerated larger particles, which is also in line with an increased ECSA (see also Table 2). Furthermore, the distribution of the NPs on the carbon support is improved as well, as indicated by the TEM micrographs.

It is known that the addition of the reducing agent during the preparation procedure controls the NP formation, which is characterized by two steps; the initial seed formation (nucleation) and the particle growth. The initial seed formation is the same in both impregnation protocols we used, but the protocols distinguish themselves in the growth phase (see experimental section). The results indicate that the stepwise addition of the precursor salts (method II) slows down the growth rate considerably, which leads to smaller NPs and higher surface area as compared to an all-at-once addition of the precursor salts, as in method I. In order to compare the dispersion of the different catalysts, we also calculated the relative dispersion of the catalysts based on the size distribution determined by SAXS and TEM. The obtained values from SAXS for the catalysts leached/PtCo/C(I), leached/PtCo/C(II), leached/HT PtCo/C(I), and leached/HT PtCo/C(II), are in good agreement with the TEM values (see also Table 1). Although the obtained values from SAXS are only a relative measure for the ECSA (corrected for the NP-C interface by assuming 50% coverage of the NPs by the substrate) the values fit well extremely well to the ECSA values we obtained in CO stripping measurements, better than the values obtained from TEM. Thus, SAXS is proved to be a very useful method for the determination of the ECSA, since uncertainties like bad contrast and local character (disadvantage for TEM) do not account here.

In addition to the size distribution, the way of adding the precursor salts also influences the Pt:Co ratio of the NPs as shown in EDS and confirmed in ICP measurements. The Pt:Co ratio obtained in the “all-at-once” method I is roughly 50:50, whereas the slower, “step-wise” method II leads to a Pt:Co ratio of 85:15 – although the same amounts of metal precursors were used in both methods. This suggests that a fast reduction rate of the precursors (method I)

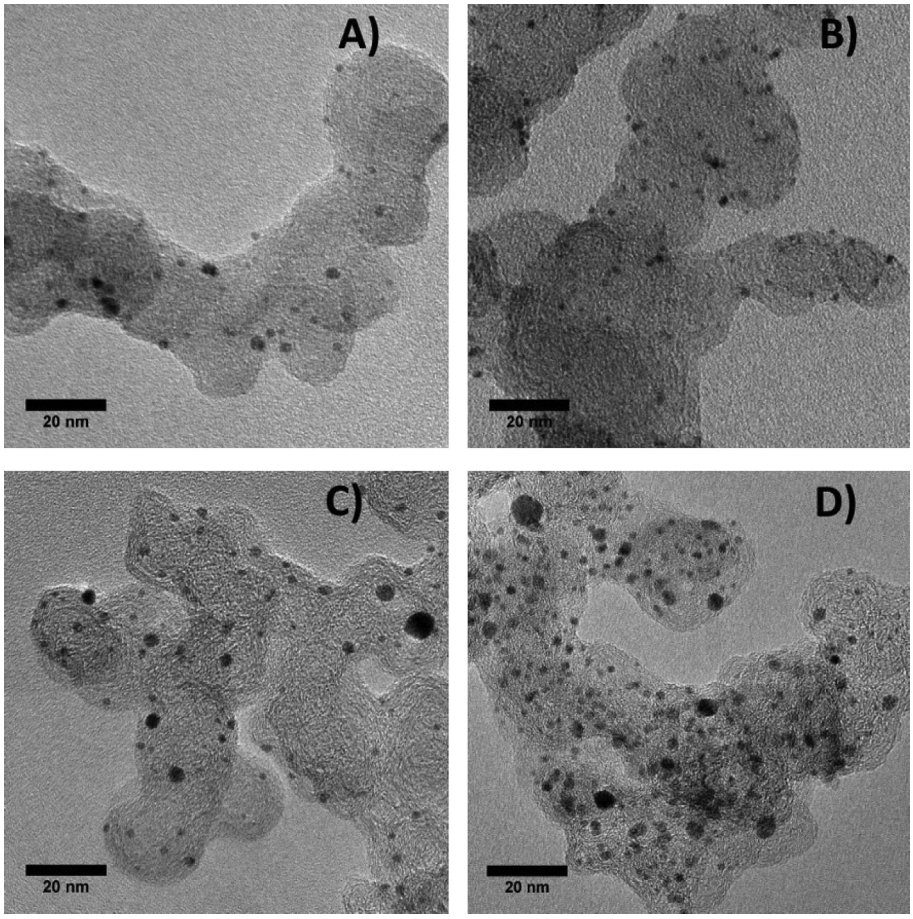

Fig. 1. TEM micrographs of Pt_xCo_{1-x}/C catalysts. A) Leached/PtCo/C(I), B) leached/PtCo/C(II), C) leached/HT PtCo/C(I), and D) leached/HT PtCo/C(II).

favours the formation of Co rich NPs. The higher reduction potential of the $PtCl_6^{2-}$/Pt redox couple (0.735 V_{SHE}) as compared to the Co^{2+}/Co couple (−0.28 V_{SHE}) indicates that the reduction of Pt is thermodynamically favourable compared to Co reduction. The addition of the reducing agent should promote the simultaneous reduction of both metals and the formation of an alloy [23]. If the reducing agent $NaBH_4$ is added in a fast manner, its access facilitates the reduction rate of Co (method I), whereas the step-wise addition decreases the Co reduction rate (method II), rendering it insufficient to reduce the whole amount of $CoCl_2 \cdot 6H_2O$, thus leading to a significantly lower Co content.

3.1.2. Influence of pre-leaching and heat treatment

It is well known that Pt_xCo_{1-x} like most Pt-alloys used for catalysing the ORR are not stable under acidic conditions [24–27], i.e. the less noble component is leached out when in contact with the electrolyte. Thus in all cases – "unleached" and "preleached" – during electrochemistry core–shell particles are formed. Following the terminology of bulk alloys, the remaining particles can be dubbed Pt_xCo_{1-x} skeleton NPs. The EDS/ICP-MS analysis demonstrates that leaching leads to a severe change in composition of the Pt_xCo_{1-x} skeleton NPs. The initial 50:50 Pt:Co ratio obtained in method I is reduced to a 86:14 composition in the skeleton NPs, whereas from the original 85:15 ratio of method II only 98:2 Cobalt atoms remain after leaching. Taking into account that dissolved metal ions have a detrimental effect on the performance of the catalyst in a membrane electrode assembly (MEA), a controlled pre-leaching of alloy catalysts before use is therefore favourable. As the electrochemical characterization of such a pre-leaching (see Table 2) shows, the removal of excess surface Co in a controlled way leads to slightly increased surface areas of the Pt_xCo_{1-x}/C powders as compared to the "electrochemical leaching" during the measurement, i.e. a more complete surface leaching.

Finally, a heat treatment of the catalysts at 500 °C in H_2 as expected leads to an increase in the particle size and a concomitant decrease in ECSA. The particle size distribution gets broader and less defined (see Fig. 2). The average particle size determined by TEM/SAXS increases from ∼2.8/1.5 nm to ∼3.4/2.4 nm and from ∼2.0/1.6 nm to ∼2.7/2.0 nm for the catalysts prepared according to method I and II respectively. The nominal composition of the catalysts remains unaffected.

3.2. Electrocatalytic properties

After having discussed the physical properties of the catalysts, we concentrate on their electrochemical properties and catalytic performance. In Fig. 3 cyclic voltammograms of the leached and heat treated catalyst samples synthesized according to methods I and II are shown, whereas in Fig. 4 a representative ORR polarization curves and corresponding Tafel plots are displayed. All characteristic properties of the catalysts as well as the ratios of the surface areas calculated both from CO striping and SAXS are summarized in Tables 1 and 2. The cyclic voltammograms are recorded in argon saturated 0.1 M $HClO_4$ solution, the polarization curves in the same electrolyte but saturated with oxygen. The cyclic voltammograms show the typical features of Pt-based catalysts with a H_{upd} region, a double layer and a potential region of oxide formation. No significant differences in the CVs of the catalysts are

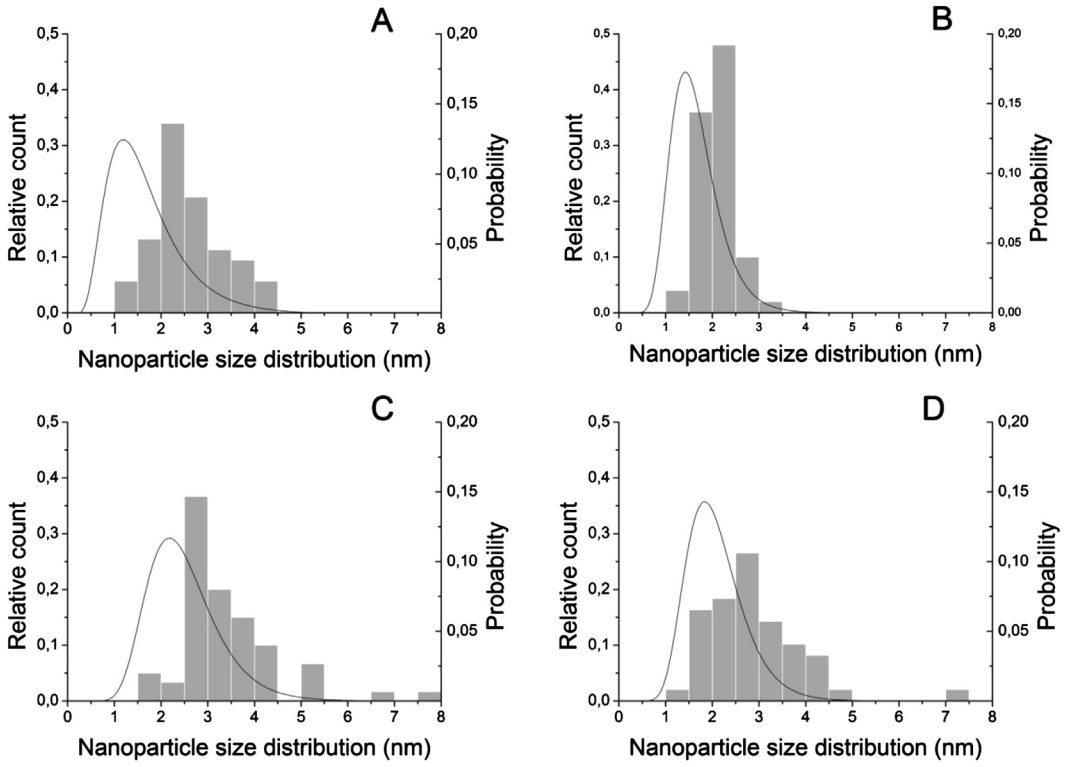

Fig. 2. Particle size distributions of carbon supported Pt_xCo_{1-x} NPs established from TEM (left scale) together with the particle size distribution obtained by SAXS. An estimate of the average particle size (diameter) is given in the brackets in nm (TEM/SAXS). A) Leached/PtCo/C(I) (~2.8/1.5), B) leached/PtCo/C(II) (~2.0/1.6), C) leached/HT PtCo/C(I) (~3.4/2.4) and D) leached/HT PtCo/C(II) (~2.74/2.0).

observed, however, the H_{upd} region reflects the different surface areas. Furthermore, the oxide formation becomes less pronounced after heat treatment. For the leached sample prepared according to method II, the reduction of oxygenated species in the negative going scan – which is often related to the ORR activity [28] – for the sample is slightly shifted to lower potentials. Following the common interpretation, such a shift would indicate a lower ORR activity as the OH coverage at fixed potential is higher than on the other samples.

Probing the ORR on the different samples, the polarization curves exhibit a region of well-defined diffusion-limited current at lower potentials, a mixed kinetic-diffusion controlled potential region suitable for extraction the ORR activity around 0.9–0.975 V_{RHE}, and terminate all at zero current at higher potentials. The parallel Tafel plots in Fig. 4B can furthermore judge the quality of the measurements.

Rather than discussing the catalytic performance of each catalyst in detail, by comparing properties of the different catalysts summarized in Table 2, we try to extract certain trends for the synthesis of optimized Pt_xCo_{1-x}/C catalysts by impregnation. As discussed before, the difference in Pt:Co ratio is the most striking difference between the two catalysts after synthesis. Nevertheless, in the as prepared state without pre-leaching, the two catalysts exhibit, within the experimental accuracy, the same specific ORR activity. That is, although the initial Co content is considerably different, this does not affect the ORR. As however the ECSA of the unleached/PtCo/C(II) catalyst is higher than the one of unleached/

Table 2
Summary of the properties of the different Pt_xCo_{1-x}/C catalysts.

Catalyst	Pt:Co ratio	ECSA ($m^2\ g_{Pt}^{-1}$)	SA_{SAxS} ($m^2\ g_{Pt}^{-1}$)	Specific activity ($mA\ cm^{-2}$)	Mass activity ($A\ mg_{Pt}^{-1}$)	Lattice constant (Å)
Pt/C data taken from Ref. [18]	100:0	76	N/A	0.49	0.37	3.925
Unleached/ PtCo/C(I)	52:48	49	N/A	0.86	0.42	N/A
Leached/ PtCo/C(I)	86:14	53	53	1.18	0.63	3.907
Leached/HT PtCo/C(I)	87:13	46	47	1.59	0.73	3.899
Unleached/ PtCo/C(II)	85:15	66	N/A	0.85	0.56	N/A
Leached/ PtCo/C(II)	98:2	68	70	1.13	0.77	3.914
Leached/ HT PtCo/ C(II)	98:2	62	57	1.32	0.82	3.912

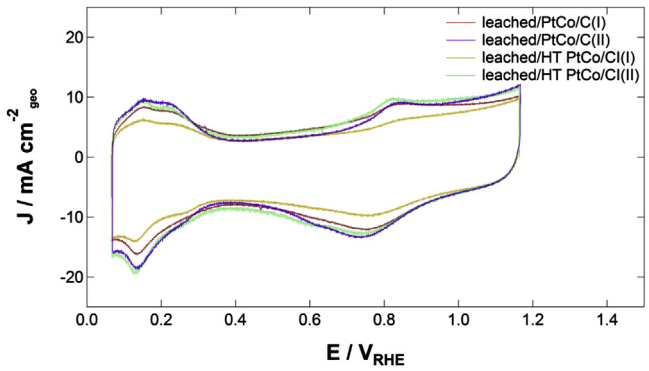

Fig. 3. Representative cyclic voltammograms of the Pt_xCo_{1-x}/C catalysts recorded at a scan rate of 50 mV s^{-1} in argon saturated 0.10 M $HClO_4$ electrolyte.

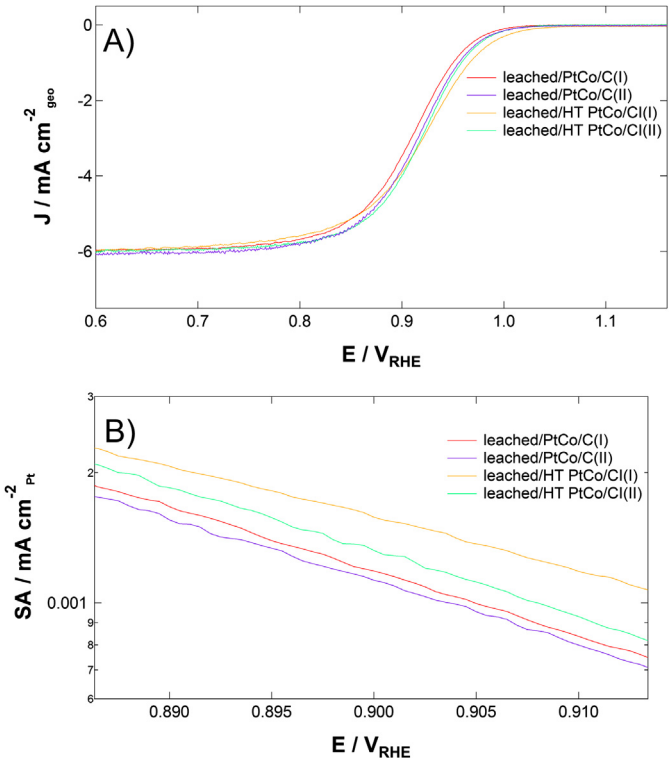

Fig. 4. A) Representative ORR polarization curves of the Pt_xCo_{1-x}/C catalysts recorded in positive going scan rate of 50 mV s^{-1} in oxygen saturated 0.1 M $HClO_4$ electrolyte; Rotation rate was 1600 rpm; B) corresponding Tafel plots of the specific activity for the ORR.

PtCo/C(I), the mass activity (MA) of the former is increased as well. The spontaneous leaching occurring during the electrochemistry [26], is a function of time and results in the change of the particle compositions which in the end are not really known. Furthermore, the leached Co in the electrolyte might have a detrimental effect on the EC.

More defined experiments are possible by pre-leaching the catalysts in a controlled way, which would be also favourable for an application of the catalysts in a MEA. Our procedure of pre-leaching shows that acid leaching drastically changes the properties of the catalysts. Both catalysts exhibit an increase in SA of about 30% due to the pre-leaching and at the same time, the ECSA slightly increases, so that the MA increases by ca. the same degree as the SA. The improvement in catalytic performance due to the controlled leaching is insofar surprising as – as mentioned earlier – a certain degree of uncontrollable leaching during the ORR measurement is unavoidable for the unleached samples as well. The difference in SA therefore might be at least partially due to contaminations released into the EC cell during the measurements of the samples that were not pre-leached. A test experiment, i.e. exchanging the electrolyte after the initial cleaning treatment (see experimental section) in exhibited indeed improved activity, however, this effect was not studied systematically as a controlled pre-leaching of the catalysts is in any case preferable.

Interestingly, the pre-leached Pt_xCo_{1-x} skeleton NPs prepared according to method I and II, still exhibit ca. the same SA, even though the Co content is also considerably different after pre-leaching. Although the activity increase in both catalysts in principle could be due to different effects, according to what is known from previous work, our findings indicate that the observed activity increase (for these particular catalysts) is mainly due to a leaching-induced strain effect rather than due to a ligand (electronic) effect, as it is expected that the latter is strongly dependent on the Pt:Co composition. The situation however changes with an additional heat treatment after pre-leaching. Then the two catalysts indeed exhibit different SA, i.e. both exhibit increased SA compared to their non-heat treated pendant, but the activity increase for the catalyst prepared according to method I is more pronounced than in the case of method II. As the ECSA is only slightly reduced due to the heat treatment, an activity increase due a sometimes proposed particle size effect [18,29,30] is unlikely and it can be assumed that the main increase in activity is due to a ligand effect initialized upon heating and alloy formation. This would explain that the activity increase induced by heat treatment is more effective if a certain amount of Co is still present in the Pt_xCo_{1-x} skeleton NPs.

4. Conclusions

To conclude, Pt_xCo_{1-x} NPs were synthesized using two variations of a modified impregnation method, where a different rate of reducing agent addition, has a detrimental effect on the structural and electrocatalytic properties of the NPs. The significant activity increase after the leaching and heat treatment in the catalysts prepared by method I, suggests that both steps are necessary to obtain a combination of strain and ligand effect. SAXS proved to be a very useful and trustworthy tool for the determination of the particle size distribution and most importantly the ECSA of the prepared catalysts, showing that this technique has many advantages compared to traditional TEM.

Summarizing the electrochemical properties of the differently prepared catalysts samples, we can rationalize our findings in the following way: in order to achieve an increased catalytic performance of Pt_xCo_{1-x} catalysts due to a strain effect a simple removal of the Co from the surface is required. Inducing this removal by pre-leaching seems definitely favourable as the activity increase is more pronounced which might be due to a poisoning effect of the released Co ions under electrochemical leaching, a larger particle strain obtained by pre-leaching, or a combination of both. By comparison, in order to induce an activity increase due to a ligand effect, a heat treatment of the catalyst is necessary. If, as in the case of method II the Co is already almost completely depleted from the NPs before the heat treatment, then the heat treatment is less effective. Therefore catalysts prepared by method I are more active after heat treatment, due to the higher Co content.

Acknowledgements

This work was supported by the Danish DFF through grant# 10-081337. We acknowledge Dipl.-Ing. Andrea Mingers of the group of Dr. Karl J.J. Mayrhofer at the MPIE for the ICP-MS analysis.

Appendix A. Supplementary data

Supplementary data related to this article can be found at http://dx.doi.org/10.1016/j.jpowsour.2013.07.023.

References

[1] T. Toda, H. Igarashi, H. Uchida, M. Watanabe, Journal of the Electrochemical Society 146 (1999) 3750–3756.
[2] V.R. Stamenkovic, B.S. Mun, M. Arenz, K.J.J. Mayrhofer, C.A. Lucas, G. Wang, P.N. Ross, N.M. Markovic, Nature Materials 6 (2007) 241–247.
[3] M. Oezaslan, M. Heggen, P. Strasser, Journal of the American Chemical Society 134 (2012) 514–524.
[4] K.J.J. Mayrhofer, V. Juhart, K. Hartl, M. Hanzlik, M. Arenz, Angewandte Chemie International Edition 48 (2009) 3529–3531.
[5] H.A. Gasteiger, N.M. Markovi&cacute, Science 324 (2009) 48–49.

[6] R. Kou, Y.Y. Shao, D.H. Wang, M.H. Engelhard, J.H. Kwak, J. Wang, V.V. Viswanathan, C.M. Wang, Y.H. Lin, Y. Wang, I.A. Aksay, J. Liu, Electrochemistry Communications 11 (2009) 954–957.
[7] M.K. Min, J.H. Cho, K.W. Cho, H. Kim, Electrochimica Acta 45 (2000) 4211–4217.
[8] F. Schuth, K. Unger, in: G. Ertl, H. Knozinger, J. Weitkamp (Eds.), Handbook of Heterogeneous Catalysis, 1997.
[9] Y. Wang, J. Ren, K. Deng, L. Gui, Y. Tang, Chemistry of Materials 12 (2000) 1622–1627.
[10] F. Kadirgan, A.M. Kannan, T. Atilan, S. Beyhan, S.S. Ozenler, S. Suzer, A. Yorur, International Journal of Hydrogen Energy 34 (2009) 9450–9460.
[11] N. Kristian, Y. Yu, J.-M. Lee, X. Liu, X. Wang, Electrochimica Acta 56 (2010) 1000–1007.
[12] J.W. Kim, J.H. Heo, S.J. Hwang, S.J. Yoo, J.H. Jang, J.S. Ha, S. Jang, T.-H. Lim, S.W. Nam, S.-K. Kim, International Journal of Hydrogen Energy 36 (2011) 12088–12095.
[13] N. Travitsky, T. Ripenbein, D. Golodnitsky, Y. Rosenberg, L. Burshtein, E. Peled, Journal of Power Sources 161 (2006) 782–789.
[14] P. Strasser, S. Koh, T. Anniyev, J. Greeley, K. More, C.F. Yu, Z.C. Liu, S. Kaya, D. Nordlund, H. Ogasawara, M.F. Toney, A. Nilsson, Nature Chemistry 2 (2010) 454–460.
[15] L. Gan, R. Yu, J. Luo, Z. Cheng, J. Zhu, The Journal of Physical Chemistry Letters 3 (2012) 934–938.
[16] K.J.J. Mayrhofer, S.J. Ashton, J. Kreuzer, M. Arenz, International Journal of Electrochemical Science 4 (2009) 1–8.
[17] K.J.J. Mayrhofer, G.K.H. Wiberg, M. Arenz, Journal of the Electrochemical Society 155 (2008) P1–P5.
[18] M. Nesselberger, S. Ashton, J.C. Meier, I. Katsounaros, K.J.J. Mayrhofer, M. Arenz, Journal of the American Chemical Society 133 (2011) 17428–17433.
[19] D.A. Stevens, S. Zhang, Z. Chen, J.R. Dahn, Carbon 41 (2003) 2769–2777.
[20] J. Speder, L. Altmann, M. Roefzaad, M. Baumer, J.J.K. Kirkensgaard, K. Mortensen, M. Arenz, Physical Chemistry Chemical Physics 15 (2013) 3602–3608.
[21] H. Borchert, E.V. Shevehenko, A. Robert, I. Mekis, A. Kornowski, G. Grubel, H. Weller, Langmuir 21 (2005) 1931–1936.
[22] V. Goertz, N. Dingenouts, H. Nirschl, Particle & Particle Systems Characterization 26 (2009) 17–24.
[23] Z. Peng, H. Yang, Nano Today 4 (2009) 143–164.
[24] E. Antolini, J.R.C. Salgado, E.R. Gonzalez, Journal of Power Sources 160 (2006) 957–968.
[25] J. Greeley, I.E.L. Stephens, A.S. Bondarenko, T.P. Johansson, H.A. Hansen, T.F. Jaramillo, J. Rossmeisl, I. Chorkendorff, J.K. Norskov, Nature Chemistry 1 (2009) 552–556.
[26] K.J.J. Mayrhofer, M. Arenz, Nature Chemistry 1 (2009) 518–519.
[27] H. Haas, M. Davis, ECS Transactions 25 (2009) 1623–1631.
[28] H.A. Gasteiger, S.S. Kocha, B. Sompalli, F.T. Wagner, Applied Catalysis B Environmental 56 (2005) 9–35.
[29] C.K. Rhee, B.J. Kim, C. Ham, Y.J. Kim, K. Song, K. Kwon, Langmuir 25 (2009) 7140–7147.
[30] H. Ye, J.A. Crooks, R.M. Crooks, Langmuir 23 (2007) 11901–11906.